Enhanced production of 3,4-dihydroxybutyrate from xylose by engineered yeast via xylonate re-assimilation under alkaline condition

Yukawa, Takahiro ; Bamba, Takahiro ; Matsuda, Mami ; Yoshida, Takanobu ; Inokuma, Kentaro ; Kim, Jungyeon ; Won Lee, Jae ; Jin, Yong-Su ;…

(Citation)
Biotechnology and Bioengineering,120(2):511-523

(Issue Date)
2023-02

(Resource Type)
journal article

(Version)
Accepted Manuscript

Title:

Enhanced production of 3,4-dihydroxybutyrate from xylose by engineered yeast via xylonate re-assimilation under alkaline condition

Authors:

Takahiro Yukawa[a], E-mail: 188p016p@stu.kobe-u.ac.jp

Takahiro Bamba[a], E-mail: t.bamba@bear.kobe-u.ac.jp

Mami Matsuda[a,b], E-mail: matsuda_mami@harbor.kobe-u.ac.jp

Takanobu Yoshida[a], E-mail: t-yoshida@port.kobe-u.ac.jp

Kentaro Inokuma[a], E-mail: kinokuma@port.kobe-u.ac.jp

Jungyeon Kim[c, d] E-mail: jungyeon@illinois.edu

Jae Won Lee[c, d] E-mail: jlee762@illinois.edu

Yong-Su Jin[c, d] E-mail: ysjin@illinois.edu

Akihiko Kondo[a, b, e] E-mail: akondo@kobe-u.ac.jp

Tomohisa Hasunuma[a, b, e], E-mail: hasunuma@port.kobe-u.ac.jp

Affiliations

[a] Graduate School of Science, Technology and Innovation, Kobe University, 1-1 Rokkodai, Nada, Kobe 657-8501, Japan

[b] Engineering Biology Research Center, Kobe University, 1-1 Rokkodai, Nada, Kobe, 657-8501, Japan

[c] Department of Food Science and Human Nutrition, University of Illinois at Urbana-Champaign, Urbana, IL, USA.

[d] Carl R. Woese Institute for Genomic Biology, University of Illinois at Urbana-Champaign, Urbana, IL, USA.

[e] RIKEN Center for Sustainable Resource Science, 1-7-22 Suehiro-cho, Tsurumi-ku, Yokohama, Kanagawa 230-0045, Japan

Corresponding author

Tomohisa Hasunuma

28 Engineering Biology Research Center, Kobe University
29 1-1 Rokkodai, Nada, Kobe 657-8501, Japan
30 hasunuma@port.kobe-u.ac.jp

31 **Funding**
32 This work was funded by project P16009 (Development of production techniques
33 for highly functional biomaterials using plant and other organism smart cells) and
34 P20011 (Development of bio-derived product production technology that
35 accelerates the realization of carbon recycling) from the New Energy and
36 Industrial Technology Development Organization (NEDO). TH was also
37 supported by Grant-in-Aid for Scientific Research (B) (JP21H01729) from the
38 Japan Society for the Promotion of Science (JSPS). TY was supported by JSPS
39 Grant-in-Aid for JSPS Fellows (JP21J10891).

40 **Abstract**
41 To realize lignocellulose-based bioeconomy, efficient conversion of xylose into
42 valuable chemicals by microbes is necessary. Xylose oxidative pathways that
43 oxidize xylose into xylonate can be more advantageous than conventional xylose
44 assimilation pathways because of fewer reaction steps without loss of carbon and
45 ATP. Moreover, commodity chemicals like 3,4-dihydroxybutyrate and 3-
46 hydroxybutyrolactone can be produced from the intermediates of xylose oxidative
47 pathway. However, successful implementations of xylose oxidative pathway in
48 yeast have been hindered because of the secretion and accumulation of xylonate
49 which is a key intermediate of the pathway, leading to low yield of target product.
50 Here, high-yield production of 3,4-dihydroxybutyrate from xylose by engineered
51 yeast was achieved through genetic and environmental perturbations.
52 Specifically, 3,4-dihydroxybutyrate biosynthetic pathway was established in yeast
53 through deletion of *ADH6* and overexpression of *ynel*. Also, inspired by the
54 mismatch of pH between host strain and key enzyme of XylD, alkaline

fermentations (pH ≥ 7.0) were performed to minimize xylonate accumulation. Under the alkaline conditions, xylonate was re-assimilated by engineered yeast and combined product yields of 3,4-dihydroxybutyrate and 3-hydroxybutyrolactone resulted in 0.791 mol/mol-xylose, which is highest compared with previous study. These results shed light on the utility of the xylose oxidative pathway in yeast.

KEYWORDS

3,4-Dihydroxybutyrate, 3-Hydroxybutyrolactone, Xylonate assimilation, Xylose oxidative pathway, *Saccharomyces cerevisiae*

1 | INTRODUCTION

For the sustainable production of commodity chemicals, replacing petrochemical-based industry with renewable biomass-based bioconversion is becoming an important proposition. Traditionally, starch and sugarcane have been used as feedstocks for microbial fermentation to produce biochemicals. However, using human-edible portions of crops may result in social and ethical issues such as unstable supply and fluctuating prices of foods. Therefore, non-edible biomass has received increasing attention as sustainable feedstocks for developing next-generation biorefineries (Protzko et al., 2018; Sun et al., 2021; Wei et al., 2013). Especially, lignocellulosic biomass, mainly composed of 30-50 % glucose, 20-25 % xylose, is one of the most abundant feedstocks on earth (Lane et al., 2018).

Glucose and xylose can be converted into various of bio-derived compounds via a conventional xylose pathway (Lee et al., 2022). However, xylose fermentation by an engineered yeast strain was much inferior to glucose fermentation because of many limiting factors such as carbon catabolite repression by glucose, redox imbalances, and by-product formation (Kim et al., 2013). In addition, conventional xylose assimilation pathway, utilizing xylose isomerase and xylose reductase/xylitol dehydrogenase, require the use of ATP when the metabolite enter central metabolic pathways such as pentose phosphate pathway (PPP) and glycolysis (Shen et al., 2020).

Recently, a xylose oxidative pathway has been identified as a novel non-phosphorylative pathway in recombinant microbial strains (Watanabe et al., 2019) (Fig. 1). The xylose oxidative pathway does not require ATP for shunting xylose into central metabolism, and the pathway is independent of the inherent glycolysis and PPP (Shen et al., 2020). As shown in Fig. 1, xylose is oxidized into 2-keto-3-deoxy-xylonate (KDX) and further converted to either α-ketoglutarate via the Weimberg pathway (Weimberg, 1961), or pyruvate and glycolaldehyde via

93 the Dahms pathway (Dahms, 1974). The xylose oxidative pathway has a potential
94 to produce chemicals such as 3,4-dihydroxybutyrate (3,4-DHBA) (Wang et al.,
95 2017), 1,2,4-butanetriol (BT) (Yukawa et al., 2021), ethylene glycol, or glycolate
96 (Salusjärvi et al., 2017) from xylose (Fig. 1).

97 3,4-DHBA and its lactonized form 3-hydroxybutyrolactone (3-HBL) are
98 versatile chemicals as 3-HBL is listed as one of the top value-added biochemicals
99 in the report by U. S. Department of Energy (Werpy and Petersen, 2004). 3-HBL
100 can be polymerized to produce polyhydroxyalkanoates, and it can be used as
101 precursors for synthesizing chiral drugs (Dhamankar et al., 2014). The microbial
102 production of 3-HBL and 3,4-DHBA from glucose and glycolate in *E. coli* was
103 firstly reported in 2013 (Martin et al., 2013), and subsequently achieved 0.32 g/L
104 of 3-HBL and 0.70 g/L of 3,4-DHBA from solely 10 g/L glucose (Dhamankar et
105 al., 2014). However, multiple reaction steps and low substrate specificity of
106 enzymes resulted in low yields and the formation of many by-products
107 (Dhamankar et al., 2014). In contrast, 3,4-DHBA production from xylose is more
108 desirable because of the 100 % theoretical yield from xylose and its
109 independence from glucose metabolism (Shen et al., 2020). Previously, 3,4-
110 DHBA synthetic pathway from xylose was established in *E. coli* (Wang et al.,
111 2017), and the integration of a fusion enzyme consisting of KDX decarboxylase
112 (PpMdlC) and xylonate dehydratase (YagF) resulted in a titer of 7.71 g/L of 3,4-
113 DHBA from 20 g/L of xylose with a molar yield of 60 % (Liu et al., 2021) (Table
114 2).

115 The xylose oxidative pathway has been introduced into bacterial strains
116 such as *Escherichia coli* (Fujiwara et al., 2020) and *Corynebacterium glutamicum*
117 (Brüsseler et al., 2019). Also, resulting strain in previous study exhibit good
118 growth from xylose as a sole carbon source (Tai et al., 2016) and product titers
119 and yields (Bai et al., 2016; Choi et al., 2016) with xylonate re-assimilation

120 (Bañares et al., 2021). The yeast *S. cerevisiae* is also desirable host strain for
121 producing cellulosic biochemicals due to its high tolerance to fermentation
122 inhibitors and no bacteriophage infection (Hong and Nielsen, 2012; Sharma et al.,
123 2022). Indeed, engineered yeast could be more suitable for the production of bio-
124 based chemicals from pretreated and hydrolyzed biomass as compared to
125 engineered *E. coli* (Bamba et al. 2019). On the other hand, the engineered yeast
126 strains accumulated excessive amounts of xylonate in the medium without
127 xylonate re-assimilation (Bamba et al., 2019, Salusjärvi et al., 2017). Xylonate
128 converted from xylose was immediately released outside the yeast cells before
129 conversion to KDX. As such, productions of target molecules by engineered *S.*
130 *cerevisiae* strains were not impressive (Salusjärvi et al., 2017; Yukawa et al.,
131 2021, Table 2). Notably, the engineered yeast strains could not grow on xylose
132 as a carbon source via Weimberg pathway (Borgström et al., 2019). These
133 studies indicate that more improvement is necessary to realize more efficient
134 xylose conversion with less xylonate accumulation via oxidative xylose pathway
135 in *S. cerevisiae*.
136 To relieve xylonate accumulation by engineered *S. cerevisiae* strain, the
137 enhancement in the activity of *Caulobacter crescentus* XylD has been needed.
138 For example, strain engineering is effective by deleting *BOL2*, encoding
139 transcriptional repressor of iron regulon, to enhance cellular iron uptake into the
140 yeast cells (Kumánovics et al., 2008). In addition to the deletion of *BOL2*, the
141 overexpression of a truncated *TYW1* (*tTYW1*), which enhances iron uptake in
142 yeast (Li et al., 2011), more improved *C. crescentus* XylD activity (Bamba et al.,
143 2019). Although the combination of *BOL2* deletion with *tTYW1* overexpression
144 further improved XylD activity *in vitro*, this genetic perturbation did not lead to a
145 higher titer of BT (Bamba et al., 2019). Although an *in vitro* enzyme assay is a
146 powerful tool to confirm the expression of an active enzymes, the improvement

147 of *in vitro* enzyme activity does not always guarantee increased expression of the
148 pathway *in vivo* or product titers. This might be due to the differences in the
149 reaction environments between *in vitro* and *in vivo*. Notably, although the optimal
150 pH range of *C. crescentus* XylD activity is reported to be from pH 7.0 to 9.0 by *in*
151 *vitro* assay (Andberg et al., 2016), *S. cerevisiae* strains harboring a xylose
152 oxidative pathway were conventionally cultivated in a pH range lower than 6.0
153 because of the acidification of the fermentation medium by the multiple factors,
154 for example, the use of ammonium ion as a nitrogen source (Hensing et al., 1995).
155 In addition, the effects of pH on xylose oxidative pathway in yeast have not been
156 reported yet.

157 Here, we demonstrated the cultivation of engineered *S. cerevisiae* with a
158 xylose oxidative pathway under weak alkaline conditions can induce extracellular
159 xylonate import to the cells, leading to the increase of the intracellular availability
160 of KDX and 3,4-DHBA production from xylose. As a result, 3,4-DHBA and 3-HBL
161 titer reached at 6.5 and 0.20 g/L from 10.9 g/L xylose with a total molar yield of
162 79.1 % without xylonate accumulation after 120 h fermentation. These results
163 demonstrate an effective strategy to reduce the accumulation of intermediates for
164 accelerating the biorefinery via the xylose oxidative pathway in yeast and provide
165 a new insight into how heterologous pathway fluxes can be altered in a host strain
166 through environmental perturbations.

167 **2 | MATERIALS AND METHODS**

168 **2.1| Chemicals**

169 Due to the commercial unavailability of (*R*)-3,4-DHBA, the 3,4-DHBA standard
170 was prepared as described in the previous study (Martin et al., 2013). 3-HBL
171 purchased from Alfa Aesar (Ward Hill, Massachusetts, USA). Xylonate and KDX
172 were purchased from Toronto Research Chemicals (North York, Canada) and
173 Sigma-Aldrich (St. Louis, MO, USA), respectively. In addition, unless otherwise

174 stated, all chemicals were purchased from Nacalai Tesque (Kyoto, Japan). 3,4-
175 Dihydroxybutanal (DHB) was identified by a capillary electrophoresis time-of-
176 flight mass spectrometry (CE-TOFMS) at *m/z* = 103.0391 due to the unavailability
177 of an authentic DHB standard.

178 **2.2 | Strains and plasmid constructions**

179 *E. coli* NovaBlue (Merck Millipore, Darmstadt, Germany) was used for plasmid
180 construction. All plasmids were constructed by using the In-fusion HD cloning kit
181 (Takara Bio USA, Mountain View, CA, USA), according to the recommended
182 protocol. Codon-optimized *C. crescentus xylB* and *xylD*, and *Lactococcus lactis*
183 *kdcA* for *S. cerevisiae* have been were previously obtained (Bamba et al., 2019).
184 Codon-optimized *E. coli ynel* and sf for *S. cerevisiae* was synthesized by Geneart
185 (Thermo Fisher Scientific, Waltham, MA, USA).

186 *S. cerevisiae* YPH499 (Stratagene, La Jolla, CA, USA) was used in this
187 study. All yeast strains used in this study and their descriptions are summarized
188 in Table 1. The details of plasmid and strain construction were specified in
189 Supplemental Text S1 and Text S2.

190 **2.3 | Shake-flask fermentation**

191 Shake flask fermentation was conducted in a 200-mL baffled Erlenmeyer flask as
192 described in the previous study (Bamba et al., 2019). Briefly, fermentation was
193 performed in 20 mL of the YPDX medium containing 10 g/L yeast extract, 20 g/L
194 Bactopeptone (Difco Laboratories),10 g/L glucose and 10 g/L xylose with an initial
195 OD_{600} = 5.0. The 1.0 mL culture was collected at every sampling point to
196 determine the amounts of metabolites.

197 **2.4 | Batch fermentation in bioreactor**

198 Batch fermentation was performed using Bio Jar.8 (ABLE Biott, Tokyo, Japan)
199 with an initial working volume of 100 mL. Yeast cells grown in 400 mL YPD
200 medium at 30 ºC were collected by centrifugation at 2,200×g for 5 min and

201 washed by 10 mL distilled water twice. The washed cells were inoculated into the
202 medium with initial OD_{600} = 5.0. The medium was composed of 10 g/L yeast
203 extract, 20 g/L Bactopeptone, 10 g/L glucose and 10 g/L xylose at 0 h. Antifoam
204 SI (FUJIFILM Wako Pure Chemical, Ltd., Osaka, Japan) was appropriately added.
205 The temperature was controlled at 30 °C. The pH of culture was maintained by
206 the automatic addition of a 5 N NaOH or 5N KOH. The airflow was maintained at
207 100 mL/min with compressed air. The culture medium was sampled every 24 h,
208 to determine metabolite concentrations and cell density (OD_{600}) using a
209 spectrophotometer.

210 **2.5 | Metabolite analysis**

211 The amounts of xylonate, BT, 3,4-DHBA and 3-HBL in the medium were analyzed
212 by GC-MS (GCMS-QP 2010 Ultra; Shimadzu, Kyoto, Japan), and the running
213 condition was described in the previous previously (Bamba et al., 2019).

214 Glucose and xylose concentrations in the medium were measured using
215 high-performance liquid chromatography (HPLC) (Shimadzu, Kyoto, Japan) with
216 a RID-10A refractive index detector (Shimadzu) equipped with an Eclipse XDB-
217 C18 column (4.6 mm × 250 mm, particle size 5 μm; Agilent Technologies,
218 Hercules, CA, USA). The HPLC system was operated at 80 °C, with a ultrapure
219 water as the mobile phase at a flow rate of 0.6 mL/min.

220 CE-TOFMS (CE, Agilent G7100; MS, Agilent G6224AA LC/MSD TOF;
221 Agilent Technologies, Palo Alto, CA, USA) was used to measure the amounts of
222 intracellular xylonate, KDX, NAD^+, $NADP^+$ and extracellular KDX analysis. The
223 method to extract metabolites from the medium (Yukawa et al., 2021) and cells
224 (Inokuma et al., 2018), and running parameters (Hasunuma et al., 2013) was
225 described in the previous reports.

226 pH in the fermentation medium was determined using compact pH meter
227 (LAQUA twin, HORIBA, Kyoto, Japan). The method of intracellular pH analysis

228 was described previously (Reifenrath & Boles, 2018), specified in Supplemental
229 Materials (Text S4).

230 **3 | RESULTS AND DISCUSSION**

231 **3.1 | A pathway design to produce 3,4-dihydroxybutyrate from xylose in**
232 **engineered yeast.**

233 The 3,4-DHBA biosynthetic pathway from xylose is based on xylose oxidative
234 pathway (Fig. 1). Xylose is converted into xylonolactone by xylose
235 dehydrogenase XylB and xylonolactone is further converted into xylonate by the
236 spontaneous reaction. Xylonate is then converted into KDX by xylonate
237 dehydratase XylD, and KDX is catalyzed into 3,4-dihydroxybutanal (DHB) by 2-
238 ketoacid decarboxylase. Previously, *Lactococcus lactis* KdcA is suitable for the
239 decarboxylation of KDX to DHB (Bamba et al., 2019). Finally, DHB is converted
240 into the 3,4-DHBA by aldehyde dehydrogenase (ALD). We first constructed the
241 BDK strain harboring one copy of *C. crescentus* XylB, XylD, and *L. lactis* KdcA
242 for the assessment of further study.

243 **3.2 | Blocking the formation of by-product 1,2,4-butanetriol in engineered**
244 ***yeast* through the knockout of alcohol dehydrogenase**

245 To construct an efficient 3,4-DHBA biosynthetic pathway with high yield from
246 xylose, the conversion of medium-chain aldehyde of DHB into a medium-chain
247 alcohol BT by endogenous enzymes in yeast needs to be eliminated (Wang et
248 al., 2017). Interruption of the reaction from DHB to yield BT would be critical
249 because substantial amounts of BT were produced in the medium as a by-
250 product by engineered *E. coli* (Wang et al., 2017). However, the enzymes
251 responsible for catalyzing this reaction in *S. cerevisiae* have not been identified
252 yet. In *S. cerevisiae*, Adh(s) catalyze the reversible reactions of aldehydes to
253 alcohols such as well-characterized Adh1 to Adh7 (de Smidt et al., 2008). For
254 example, Adh6 and Adh7 are known to exhibit broad substrate specificities

255 (Larroy et al., 2002a; Larroy et al., 2002b). Although substrate specificities of
256 Adh(s) in *S. cerevisiae* have been investigated, no ADH(s) is known to recognize
257 unnatural compounds such as DHB (Niu et al., 2003).

258 In order to reduce the formation of BT, we screened Adh(s) enzymes that
259 might catalyze BT formation by disrupting each *ADH* genes in the BDK strain. To
260 construct a *ADH* deletion library, each *ADH* gene from *ADH1* to *ADH7* was
261 disrupted in the BDK strain, respectively. We performed glucose and xylose co-
262 fermentation and examined the xylose consumption and BT production by the
263 ADH disrupted strain (Fig. 2A and 2B). The parental BDK strain produced 0.22
264 g/L of BT from 10.6 g/L xylose at 96 h (Fig. 2A and 2B). Deletion of *ADH2, ADH5,*
265 or *ADH7* did not change the titers of BT. Interestingly, the deletion of *ADH3* had
266 a positive effect on BT production, and the BT titer reached 0.29 g/L after 96 h
267 fermentation (Fig. 2B). In contrast, the deletion of *ADH1*, *ADH4*, and *ADH6*
268 reduced the titers of BT after 96 h fermentation as compared with the parental
269 BDK strain. In particular, the BDKΔ6 with the deletion of *ADH6* produced BT only
270 at 0.01 g/L (Fig. 2B). Deletion of *ADH1* also reduced the xylose consumption (Fig.
271 2A), leading to the low BT production (Fig. 2B). Deletion of *ADH4* also reduced
272 BT titer at 0.18 g/L (Fig. 2B). In particular, the titer of BT was dropped from 0.22
273 g/L of BDK strain to 0.01 g/L of BDKΔ6 strain at 96 h by the deletion of *ADH6*
274 (Fig. 2B). These results suggest that *ADH6* is a deletion target for a high yield
275 production of 3,4-DHBA by engineered yeast. However, the BDKΔ6 strain did not
276 produce 3,4-DHBA. This suggested further engineering is required for 3,4-DHBA
277 production.

278 **3.3 | Increased fluxes from xylonate to 3,4-dihydroxybutanal enable the**
279 **production of 3,4-dihydroxybutyrate in engineered yeast**

280 Previously, we developed the BDδK603 strain for the production of BT (Yukawa
281 et al., 2021). This strain harbors one copy of *C. crescentus* XylB and XylD, and

282 six copies of *L. lactis* KdcA. In addition, iron metabolism was modified with the
283 deletion of *BOL2* and the overexpression of *tTYW1* to improve the activity of iron-
284 sulfur protein XylD (Bamba et al., 2019; Yukawa et al., 2021). As the BDδK603
285 strain exhibits higher fluxes from xylose to DHB (Yukawa et al., 2021), we
286 reasoned that the deletion of *ADH6* in the BDδK603 strain might enable the
287 production of 3,4-DHBA from xylose.

288 To minimize BT formation while keeping the flux of xylose to DHB in the
289 BDδK603 strain, *ADH6 gene* was deleted in the genome of the BDδK603 strain,
290 resulting in the construction of the BDδK604 strain. We examined the product
291 profiles from glucose and xylose fermentation by the parental BDδK603 strain
292 and *ADH6*-deleted BDδK604 strains. The BDδK603 strain produced 7.4 g/L of
293 xylonate (Fig. S1) and 1.5 g/L of BT (Fig. 2C). Interestingly, the BDδK603 strain
294 produced 0.3 g/L of 3,4-DHBA without the deletion of any *ADH(s)* or integration
295 of ALD catalyzing the reaction from DHB to 3,4-DHBA (Fig. 2D). By the disruption
296 of *ADH6*, the BDδK604 strain produced 8.2 g/L of xylonate (Fig. S1), 0.3 g/L of
297 BT (Fig. 2C), and 0.4 g/L of 3,4-DHBA (Fig. 2D). While the deletion of *ADH6*
298 reduced BT formation from 1.5 to 0.3 g/L of BT (Fig. 2C), the improvement of 3,4-
299 DHBA production was marginal (Fig. 2D, 0.3 vs. 0.4 g/L of 3,4-DHBA) between
300 the BDδK603 and BDδK604 strains. The molar yield of 3,4-DHBA in BDδK604
301 strain was only 0.02 %. While endogenous aldehyde dehydrogenase in yeast
302 might be converting DHB to 3,4-DHBA (Fig. 2D), heterologous enzyme needs to
303 be introduced into the BDδK604 strain for the enhanced production of 3,4-DHBA.

304 **3.4 | Improvement of 3,4-dihydroxybutyrate production by integration of**
305 **suitable aldehyde dehydrogenase**

306 As the structure of DHB is similar to that of succinate semialdehyde, succinate
307 semialdehyde dehydrogenase YneI from *E. coli* was overexpressed to the
308 increased production of the 3,4-DHBA by engineered *E. coli* (Wang et al., 2017).

309 Thus, the *yneI* was selected as a target gene for the enhanced production of 3,4-
310 DHBA in *S. cerevisiae*. In addition, we reasoned that endogenous enzymes in *S*
311 *cerevisiae* such as succinate semialdehyde dehydrogenase of Uga2, NAD^+-
312 dependent cytoplasmic ALDs of Ald2 and Ald3 might be responsible for the small
313 amounts of 3,4-DHBA produced by the BDδK603 and BDδK604 strains (Fig. 2D).
314 Therefore, Uga2, Ald2, and Ald3 were additionally selected as candidate
315 enzymes for 3,4-DHBA production.

316 Each gene of *yneI*, *UGA2*, *ALD2* and *ALD3* under the control of *TDH3*
317 promoter was integrated into the BDδK604 strain, resulting in the construction of
318 the BDδK604-YneI, BDδK604-Uga2, BDδK604-Ald2 and BDδK604-Ald3 strains,
319 respectively. As shown in Fig. 3A, the overexpression of *yneI* enhanced 3,4-
320 DHBA production at 1.0 g/L from 10.6 g/L of consumed xylose (Fig. S2) with a
321 molar yield of 11.8 %, which was 2.5-fold higher than the parental strain BDδK604
322 at 0.4 g/L (Fig. 2D). The overexpression of *UGA2* did not improve the 3,4-DHBA
323 titer. The overexpression of *ALD2* and *ALD3* also enhanced the carbon flux
324 toward 3,4-DHBA, producing 0.7 and 0.5 g/L of 3,4-DHBA by the BDδK604-Ald2
325 and BDδK604-Ald3 strains, respectively. These results suggested that YneI is
326 the most effective ALD among the overexpressed enzymes.

327 Xylonate accumulation by these strains changed marginally, but the
328 overexpression of *yneI* relieved xylonate accumulation at 8.2 g/L (Fig. 3B). This
329 means that 66.5% of the consumed xylose was wasted into the medium as
330 xylonate, resulting in the low yield of 3,4-DHBA from xylose by the BDδK604-
331 YneI strain. BT formation by the BDδK604-YneI strain was slightly lower as
332 compared with those by the other strains, and intracellular pH values and the pool
333 size of intracellular NAD^+ and $NADP^+$ at 24 h did not exhibit significant differences
334 (Fig. S3). Thus, YneI might have a better substrate specificity for DHB between
335 the four enzymes. In addition to the change of metabolites, pH of the culture

336 medium of the BDδK604-YneI strain drastically dropped from pH = 6.3 at 0 h to
337 pH = 4.0 at 96 h (Fig. 3C) because a major by-product xylonate is a weak acid
338 and is known to acidify fermentation media (Toivari et al., 2012), and final product
339 3,4-DHBA is also weak acid with a pKa value of 4.09.

340 **3.5 | The 3,4-dihydroxybutyrate production under the pH control**

341 Control of oxygen supply and pH of culture media in a lab-scale shake-flask
342 fermentation is difficult so that our fermentation results for the production of 3,4-
343 DHBA might not reflect the full potential of the engineered BDδK604-YneI strains.
344 As such, pH-controlled fermentation in a bioreactor were performed to examine
345 the production capacity of 3,4-DHBA production by the BDδK604-YneI under
346 different aeration conditions.

347 Using a bioreactor, fermentation was performed while keeping the lower
348 limit of pH of the medium was kept at 6.0 by NaOH. The effects of aeration on
349 the production of 3,4-DHBA by the BDδK604-YneI were evaluated through
350 changing agitation speeds from 200 to 500 rpm. Dissolved oxygen levels were
351 controlled corresponding to the agitation speeds (Fig. S4). Glucose was
352 completely consumed within 24 h by each agitation speed (Fig. S5), and xylose
353 was sequentially consumed in the fermentation at 500 rpm (Fig. 4A). 5.8 g/L of
354 xylonate was accumulated (Fig. 4B) and 3.5 g/L of 3,4-DHBA was produced (Fig.
355 4C). Compared to the result at 500 rpm, fermentations at lower agitation speeds
356 exhibited the reduced xylose consumption rates, less amounts of accumulated
357 xylonate, and higher titers of 3,4-DHBA. Notably, the fermentation at 300 rpm
358 produced 4.6 g/L of 3,4-DHBA with a molar yield of 51.3 % from 11.2 g/L of xylose.
359 Increase in the production of 3,4-DHBA under low aeration conditions at 300 rpm
360 would be due to the XylD activity. XylD is known to be IlvD/EDD protein family
361 requires an iron-sulfur cluster for its activity (Andberg et al., 2016). Functional
362 expression of prokaryotic iron-sulfur proteins in yeast *S. cerevisiae* has been so

363 difficult because of oxygen sensibility of iron-sulfur proteins (Kirby et al. 2016), or
364 conceivably low availability of iron-sulfur cluster (Bamba et al. 2019). Lower
365 agitation speeds might reduce the loss of function of XylD, leading to less
366 xylonate accumulation and increased the production of 3,4-DHBA even with
367 lower xylose consumption.

368 Importantly, 3-HBL was also produced from xylose by spontaneous
369 cyclization at 0.64 (200 rpm), 0.49 (300 rpm), 0.40 (400 rpm), and 0.39 g/L (500
370 rpm) under each agitation speed, respectively (Fig. 4D). This is the first report of
371 3-HBL production from xylose in *S. cerevisiae*, to the best of our knowledge. The
372 previous study showed the dual production of 3,4-DHBA and 3-HBL from glucose
373 (Dhamankar et al., 2014), but did not confirm the production of 3-HBL from xylose
374 (Gao et al., 2017; Liu et al., 2021; Wang et al., 2017).

375 **3.6 | Xylonate re-assimilation led to enhanced 3,4-dihydroxybutyrate**
376 **production by engineered yeast**

377 The beneficial effects of the pH and agitation control on 3,4-DHBA production
378 were confirmed. While xylonate accumulation reduced with the control of pH and
379 aeration, 4.8 g/L of xylonate was still accumulated with the molar yield of 38.7 %
380 of the consumed xylose. Previously, *C. crescetus* XylD activity was determined
381 to be highly active under a weak alkaline condition at pH = 8.5 (Andberg et al.,
382 2016). The optimal pH for XylD was narrow so that XylD activities drastically
383 dropped when pH was lower than 8.5. However, in previous studies, engineered
384 yeast strains harboring a xylose oxidative pathway with *C. crescentus* XylD have
385 been empirically cultivated at pH ≤ 6.0 (Bamba et al., 2019; Borgström et al.,
386 2019; Salusjärvi et al., 2017). As the intracellular pH of *S. cerevisiae* responds to
387 the extracellular pH changes (Orij et al., 2009), traditional yeast fermentation at
388 pH ≤ 6.0 might make XylD inactive in *S. cerevisiae*. A weak alkaline environment
389 would enhance the heterologous XylD activity by elevating intracellular pH in *S.*

390 *cerevisiae*. However, the impacts of alkaline fermentation on xylose oxidative
391 metabolism in *S. cerevisiae* have never been investigated so far.
392 To resolve the pH mismatch between optimal yeast growth and XylD
393 activity, fermentations were performed while keeping a lower limit of pH in the
394 medium at pH ≥ 7.0 or pH ≥ 8.0 by NaOH or KOH. To control the pH in the
395 fermentation medium, NaOH or KOH was used. Glucose was consumed within
396 24 h under all fermentation conditions (Fig. 5A). On the other hand, xylose
397 consumption rates reduced when the pH was maintained at pH ≥ 8.0 as
398 compared to when the pH was maintained at pH ≥ 7.0 (Fig. 5B). Interestingly,
399 xylonate was re-assimilated from the medium into the cells under alkaline
400 conditions and completely re-assimilated after 120 h cultivation. (Fig. 5C). This is
401 the first observation of xylonate re-assimilation when using *S. cerevisiae* as a
402 host strain. In all fermentations conducted under alkaline conditions, the titers of
403 3,4-DHBA increased up to 6.5 g/L with a molar yield of 74.5 % from 10. 9 g/L of
404 xylose when pH was controlled at pH ≥ 8.0 using KOH (Fig. 5D). These results
405 indicated that the weak alkaline conditions might lead to the *in vivo* activation of
406 *C. crescentus* XylD, the re-assimilations of xylonate, and the increased
407 productions of 3,4-DHBA production. For the efficient construction of
408 heterologous pathway, researchers need to reconsider how heterologous
409 enzymes are expressed in active form inside the microbial cells by the matching
410 the optimal pH between host strain and target enzymes since the active pH range
411 of heterologous enzymes often differs from the optimal pH of microbial host
412 strains (Ahn et al., 2020). Unfortunately, 3-HBL production was decreased to 0.30
413 (NaOH, pH ≥ 7.0), 0.21 (NaOH, pH ≥ 8.0), 0.37 (KOH, pH ≥ 7.0), and 0.20 g/L
414 (KOH, pH ≥ 8.0) under alkaline conditions (Fig. S7). as compared to 0.49 g/L of
415 3-HBL in the fermentation conducted at pH ≥ 6.0 using NaOH (Fig. 4D).

416 To elucidate the detailed metabolome in the 3,4-DHBA synthetic pathway,
417 the intracellular amounts of xylonate, KDX and DHB, and extracellular amounts
418 of KDX were measured. The intracellular amount of xylonate did not change
419 under each fermentation conditions except for the intracellular xylonate at pH ≥
420 8.0 using KOH (Fig. 6A). In contrast, the intracellular levels of KDX and DHB were
421 increased remarkably when the cells were cultured at pH ≥ 8.0 (Fig. 6B and 6C),
422 which could be due to increased XylD activity dependent on the higher
423 intracellular pH values. Indeed, lifting the pH in the medium from pH 6.0 to 8.0
424 led to the increase in intracellular pH values, and XylD activity was dependent on
425 pH from 6.0 to 8.0 (Fig. S6). Consistent with the increased level of intracellular
426 KDX, the extracellular amount of KDX was also increased when the cells were
427 cultured at pH ≥ 7.0 or at pH ≥ 8.0 (Fig. 6D). This indicated that putative
428 bottlenecks in the 3,4-DHBA biosynthetic pathway might be the reaction from
429 KDX to DHB. The expression levels of the genes involved in the 3,4-DHBA
430 synthetic pathway did not change by changing the pH to alkaline conditions
431 except for *xylD* (Fig. S8). Hence, this would be caused by the mismatch of the
432 optimal pH between enzymes. For example, the optimal pH of *L. lactis* KdcA is
433 pH 6.0 (Yep et al., 2006), which is quite different from those of *C. cresrentus* XylB
434 (pH 9.0) (Toivari et al., 2012), *C. cresrentus* XylD (pH 8.5) (Andberg et al., 2016).
435 Although the pH dependency of *E. coli* YneI has not been reported, the enzyme
436 is assayed at pH = 7.8 (Fuhrer et al., 2007). Thus, a weak alkaline environment
437 would not be beneficial for all the reactions in the biosynthetic pathway.
438 When KOH was used as an alkaline reagent, xylonate accumulation was
439 lower as compared to when NaOH was used (Fig. 5C). However, it did not have
440 an impact on the 3,4-DHBA production. This might be caused by the low flux in
441 the 3,4-DHBA biosynthetic pathway, leading to the accumulation of intermediates
442 of KDX and DHB. After 72 h cultivation, intracellular levels of KDX and DHB when

443 KOH was used was 2.1- and 1.5-fold higher than those in the fermentation using
444 NaOH at pH ≥ 7.0 (Fig. 6A and 6B). Moreover, KDX when using KOH was
445 accumulated in the medium with 1.5-fold higher as compared to using NaOH (Fig.
446 6C). Thus, the flux in the 3,4-DHBA biosynthetic pathway needs to be improved
447 for further study.

448 In addition to the effects of pH, transporters involved in facilitating the
449 import or export across the yeast cell membranes need to be identified for further
450 engineering. For example, *S. cerevisiae* transports weak carboxylic acids like
451 acetate into the cells, and the Jen family proteins, belong to the major facilitator
452 superfamily, are identified to associate with plasma membrane transport of weak
453 carboxylic acids in yeast (Giannattasio et al., 2013). When proteins involved in
454 the transport of DHB, KDX and 3,4-DHBA are identified, further engineering could
455 realize more efficient production of 3,4-DHBA with less accumulation of the
456 intermediates.

457 **4 |CONCLUSIONS**

458 This research demonstrated xylonate re-assimilation by engineered
459 yeast for the first time. The alkaline environment is the trigger of xylonate re-
460 assimilation, overcoming the low yields of a xylose derivative chemicals. Based
461 on this study, we envision the implementation of a xylose oxidative pathway in
462 yeast would be more accelerated and universally used to produce biofuels and
463 biochemicals from lignocellulosic feedstock. Furthermore, these results provide
464 new insights into the reduction and re-assimilation of intermediates, as well as
465 how the heterologous pathway works in the host strain to match the active pH
466 range of host strain and target enzyme.

467

468 **REFERENCE**

469 Ahn, J. H., Seo, H., Park, W., Seok, J., Lee, J. A., Kim, W. J., Kim, G. B., Kim,
470 K.-J., & Lee, S. Y. (2020). Enhanced succinic acid production by *Mannheimia*
471 employing optimal malate dehydrogenase. *Nature Communications, 11(1)*, 1970.
472 https://doi.org/10.1038/s41467-020-15839-z

473 Andberg, M., Aro-Kärkkäinen, N., Carlson, P., Oja, M., Bozonnet, S., Toivari, M.,
474 Hakulinen, N., O'Donohue, M., Penttilä, M., & Koivula, A. (2016).
475 Characterization and mutagenesis of two novel iron–sulphur cluster pentonate
476 dehydratases. *Applied Microbiology and Biotechnology, 100(17)*, 7549–7563.
477 https://doi.org/10.1007/s00253-016-7530-8

478 Bai, W., Tai, Y.-S., Wang, J., Wang, J., Jambunathan, P., Fox, K. J., & Zhang, K.
479 (2016). Engineering nonphosphorylative metabolism to synthesize mesaconate
480 from lignocellulosic sugars in *Escherichia coli. Metabolic Engineering, 38*, 285–
481 292. https://doi.org/10.1016/j.ymben.2016.09.007

482 Bamba, T., Yukawa, T., Guirimand, G., Inokuma, K., Sasaki, K., Hasunuma, T.,
483 & Kondo, A. (2019). Production of 1,2,4-butanetriol from xylose by
484 *Saccharomyces cerevisiae* through Fe metabolic engineering. *Metabolic*
485 *Engineering, 56*, 17–27. https://doi.org/10.1016/j.ymben.2019.08.012

486 Bañares, A. B., Nisola, G. M., Valdehuesa, K. N. G., Lee, W.-K., & Chung, W.-J.
487 (2021). Understanding D-xylonic acid accumulation: A cornerstone for better
488 metabolic engineering approaches. *Applied Microbiology and Biotechnology,*
489 *105(13)*, 5309–5324. https://doi.org/10.1007/s00253-021-11410-y

490 Borgström, C., Wasserstrom, L., Almqvist, H., Broberg, K., Klein, B., Noack, S.,
491 Lidén, G., & Gorwa-Grauslund, M. F. (2019). Identification of modifications
492 procuring growth on xylose in recombinant *Saccharomyces cerevisiae* strains
493 carrying the Weimberg pathway. *Metabolic Engineering, 55*, 1–11.
494 https://doi.org/10.1016/j.ymben.2019.05.010

Brüsseler, C., Späth, A., Sokolowsky, S., & Marienhagen, J. (2019). Alone at last! – Heterologous expression of a single gene is sufficient for establishing the five-step Weimberg pathway in *Corynebacterium glutamicum*. *Metabolic Engineering Communications, 9,* e00090. https://doi.org/10.1016/j.mec.2019.e00090

Calahorra, M., Martínez, G. A., Hernández-Cruz, A., & Peña, A. (1998). Influence of monovalent cations on yeast cytoplasmic and vacuolar pH. *Yeast, 14(6)*, 501–515. https://doi.org/10.1002/(SICI)1097-0061(19980430)14:6<501::AID-YEA249>3.0.CO;2-6

Choi, S. Y., Park, S. J., Kim, W. J., Yang, J. E., Lee, H., Shin, J., & Lee, S. Y. (2016). One-step fermentative production of poly(lactate-co-glycolate) from carbohydrates in Escherichia coli. *Nature Biotechnology, 34(4)*, 435–440. https://doi.org/10.1038/nbt.3485

Dahms, A.S., (1974). 3-Deoxy-D-pentulosonic acid aldolase and its role in a new pathway of D-xylose degradation. Biochem. Biophys. *Res. Commun. 60*, 1433–1439

de Smidt, O., du Preez, J. C., & Albertyn, J. (2008). The alcohol dehydrogenases of *Saccharomyces cerevisiae*: A comprehensive review. *FEMS Yeast Research, 8(7)*, 967–978. https://doi.org/10.1111/j.1567-1364.2008.00387.x

Dhamankar, H., Tarasova, Y., Martin, C. H., & Prather, K. L. J. (2014). Engineering E. coli for the biosynthesis of 3-hydroxy-γ-butyrolactone (3HBL) and 3,4-dihydroxybutyric acid (3,4-DHBA) as value-added chemicals from glucose as a sole carbon source. *Metabolic Engineering, 25*, 72–81. https://doi.org/10.1016/j.ymben.2014.06.004

Fuhrer, T., Chen, L., Sauer, U., & Vitkup, D. (2007). Computational Prediction and Experimental Verification of the Gene Encoding the NAD^+/$NADP^+$-Dependent Succinate Semialdehyde Dehydrogenase in *Escherichia coli*. *Journal of Bacteriology, 189(22)*, 8073–8078. https://doi.org/10.1128/JB.01027-07

522 Fujiwara, R., Noda, S., Tanaka, T., & Kondo, A. (2020). Metabolic engineering of
523 *Escherichia coli* for shikimate pathway derivative production from glucose–xylose
524 co-substrate. *Nature Communications, 11(1)*, 279.
525 https://doi.org/10.1038/s41467-019-14024-1
526 Gao, H., Gao, Y., & Dong, R. (2017). Enhanced biosynthesis of 3,4-
527 dihydroxybutyric acid by engineered *Escherichia coli* in a dual-substrate system.
528 *Bioresource Technology, 245*, 794–800.
529 https://doi.org/10.1016/j.biortech.2017.09.017
530 Giannattasio, S., Guaragnella, N., Ždralević, M., & Marra, E. (2013). Molecular
531 mechanisms of *Saccharomyces cerevisiae* stress adaptation and programmed
532 cell death in response to acetic acid. *Frontiers in Microbiology*, 4.
533 https://doi.org/10.3389/fmicb.2013.00033
534 Hasunuma, T., Kikuyama, F., Matsuda, M., Aikawa, S., Izumi, Y., & Kondo, A.
535 (2013). Dynamic metabolic profiling of cyanobacterial glycogen biosynthesis
536 under conditions of nitrate depletion. *Journal of Experimental Botany, 64(10)*,
537 2943–2954. https://doi.org/10.1093/jxb/ert134
538 Hensing, M. C. M., Bangma, K. A., Raamsdonk, L. M., de Hulster, E., van Dijken,
539 J. P., & Pronk, J. T. (1995). Effects of cultivation conditions on the production of
540 heterologous α-galactosidase by *Kluyveromyces lactis*. *Applied Microbiology and*
541 *Biotechnology, 43(1)*, 58–64. https://doi.org/10.1007/BF00170623
542 Hong, K.-K., & Nielsen, J. (2012). Metabolic engineering of *Saccharomyces*
543 *cerevisiae*: A key cell factory platform for future biorefineries. Cellular and
544 *Molecular Life Sciences, 69(16)*, 2671–2690. https://doi.org/10.1007/s00018-
545 012-0945-1
546 Inokuma, K., Matsuda, M., Sasaki, D., Hasunuma, T., & Kondo, A. (2018).
547 Widespread effect of N-acetyl-d-glucosamine assimilation on the metabolisms of

548 amino acids, purines, and pyrimidines in *Scheffersomyces stipitis*. *Microbial Cell*
549 *Factories, 17*. https://doi.org/10.1186/s12934-018-0998-4
550 Kim, S. R., Park, Y.-C., Jin, Y.-S., & Seo, J.-H. (2013). Strain engineering of
551 *Saccharomyces cerevisiae* for enhanced xylose metabolism. *Biotechnology*
552 *Advances, 31(6)*, 851–861. https://doi.org/10.1016/j.biotechadv.2013.03.004
553 Kirby, J., Dietzel, K. L., Wichmann, G., Chan, R., Antipov, E., Moss, N., Baidoo,
554 E. E. K., Jackson, P., Gaucher, S. P., Gottlieb, S., LaBarge, J., Mahatdejkul, T.,
555 Hawkins, K. M., Muley, S., Newman, J. D., Liu, P., Keasling, J. D., & Zhao, L.
556 (2016). Engineering a functional 1-deoxy-D-xylulose 5-phosphate (DXP) pathway
557 in *Saccharomyces cerevisiae*. *Metabolic Engineering,* 38, 494–503.
558 https://doi.org/10.1016/j.ymben.2016.10.017
559 Kumánovics, A., Chen, O. S., Li, L., Bagley, D., Adkins, E. M., Lin, H., Dingra, N.
560 N., Outten, C. E., Keller, G., Winge, D., Ward, D. M., & Kaplan, J. (2008).
561 Identification of *FRA1* and *FRA2* as Genes Involved in Regulating the Yeast Iron
562 Regulon in Response to Decreased Mitochondrial Iron-Sulfur Cluster Synthesis.
563 *Journal of Biological Chemistry, 283(16)*, 10276–10286.
564 https://doi.org/10.1074/jbc.M801160200
565 Lane, S., Dong, J., & Jin, Y.-S. (2018). Value-added biotransformation of
566 cellulosic sugars by engineered *Saccharomyces cerevisiae*. *Bioresource*
567 *Technology, 260*, 380–394. https://doi.org/10.1016/j.biortech.2018.04.013
568 Larroy, C., Fernández, M. R., González, E., Parés, X., & Biosca, J. A. (2002).
569 Characterization of the *Saccharomyces cerevisiae* YMR318C (*ADH6*) gene
570 product as a broad specificity NADPH-dependent alcohol dehydrogenase:
571 Relevance in aldehyde reduction. *Biochemical Journal, 361(Pt 1)*, 163–172.
572 Larroy, C., Parés, X., & Biosca, J. A. (2002). Characterization of a
573 *Saccharomyces cerevisiae* NADP(H)-dependent alcohol dehydrogenase
574 (ADHVII), a member of the cinnamyl alcohol dehydrogenase family. *European*

575 *Journal of Biochemistry, 269(22)*, 5738–5745. https://doi.org/10.1046/j.1432-
576 1033.2002.03296.x
577 Lee, Y., Kim, C., Sun, L., Lee, T., & Jin, Y. (2022). Selective production of retinol
578 by engineered *Saccharomyces cerevisiae* through the expression of retinol
579 dehydrogenase. *Biotechnology and Bioengineering, 119(2)*, 399–410.
580 https://doi.org/10.1002/bit.28004
581 Li, L., Jia, X., Ward, D. M., & Kaplan, J. (2011). Yap5 Protein-regulated
582 Transcription of the *TYW1* Gene Protects Yeast from High Iron Toxicity. The
583 *Journal of Biological Chemistry, 286(44)*, 38488–38497.
584 https://doi.org/10.1074/jbc.M111.286666
585 Liu, Y., Mao, X., Zhang, B., Lin, J., & Wei, D. (2021). Modification of an
586 engineered *Escherichia coli* by a combinatorial strategy to improve 3,4-
587 dihydroxybutyric acid production. *Biotechnology Letters, 43(10)*, 2035–2043.
588 https://doi.org/10.1007/s10529-021-03169-z
589 Martin, C. H., Dhamankar, H., Tseng, H.-C., Sheppard, M. J., Reisch, C. R., &
590 Prather, K. L. J. (2013). A platform pathway for production of 3-hydroxyacids
591 provides a biosynthetic route to 3-hydroxy-γ-butyrolactone. *Nature*
592 *Communications, 4(1)*. https://doi.org/10.1038/ncomms2418
593 Niu, W., Molefe, M. N., & Frost, J. W. (2003). Microbial Synthesis of the Energetic
594 Material Precursor 1,2,4-Butanetriol. 2.
595 Orij, R., Postmus, J., Ter Beek, A., Brul, S., & Smits, G. J. (2009). *In vivo*
596 measurement of cytosolic and mitochondrial pH using a pH-sensitive GFP
597 derivative in *Saccharomyces cerevisiae* reveals a relation between intracellular
598 pH and growth. *Microbiology, 155(1)*, 268–278.
599 https://doi.org/10.1099/mic.0.022038-0
600 Peña, A., Sánchez, N. S., Álvarez, H., Calahorra, M., & Ramírez, J. (2015).
601 Effects of high medium pH on growth, metabolism and transport in

602 *Saccharomyces cerevisiae*. *FEMS Yeast Research, 15(2)*.
603 https://doi.org/10.1093/femsyr/fou005
604 Protzko, R. J., Latimer, L. N., Martinho, Z., de Reus, E., Seibert, T., Benz, J. P.,
605 & Dueber, J. E. (2018). Engineering *Saccharomyces cerevisiae* for co-utilization
606 of d-galacturonic acid and d-glucose from citrus peel waste. *Nature*
607 *Communications, 9(1)*. https://doi.org/10.1038/s41467-018-07589-w
608 Reifenrath, M., & Boles, E. (2018). A superfolder variant of pH-sensitive pHluorin
609 for *in vivo* pH measurements in the endoplasmic reticulum. *Scientific Reports*,
610 8(1), 11985. https://doi.org/10.1038/s41598-018-30367-z
611 Salusjärvi, L., Toivari, M., Vehkomäki, M.-L., Koivistoinen, O., Mojzita, D.,
612 Niemelä, K., Penttilä, M., & Ruohonen, L. (2017). Production of ethylene glycol
613 or glycolic acid from D-xylose in *Saccharomyces cerevisiae*. *Applied Microbiology*
614 *and Biotechnology*, *101(22)*, 8151–8163. https://doi.org/10.1007/s00253-017-
615 8547-3
616 Sharma, J., Kumar, V., Prasad, R., & Gaur, N. A. (2022). Engineering of
617 *Saccharomyces cerevisiae* as a consolidated bioprocessing host to produce
618 cellulosic ethanol: Recent advancements and current challenges. *Biotechnology*
619 *Advances, 56*, 107925. https://doi.org/10.1016/j.biotechadv.2022.107925
620 Shen, L., Kohlhaas, M., Enoki, J., Meier, R., Schönenberger, B., Wohlgemuth, R.,
621 Kourist, R., Niemeyer, F., van Niekerk, D., Bräsen, C., Niemeyer, J., Snoep, J.,
622 & Siebers, B. (2020). A combined experimental and modelling approach for the
623 Weimberg pathway optimization. *Nature Communications, 11(1)*, 1098.
624 https://doi.org/10.1038/s41467-020-14830-y
625 Sun, L., Lee, J. W., Yook, S., Lane, S., Sun, Z., Kim, S. R., & Jin, Y.-S. (2021).
626 Complete and efficient conversion of plant cell wall hemicellulose into high-value
627 bioproducts by engineered yeast. *Nature Communications, 12(1)*, 4975.
628 https://doi.org/10.1038/s41467-021-25241-y

Tai, Y.-S., Xiong, M., Jambunathan, P., Wang, J., Wang, J., Stapleton, C., & Zhang, K. (2016). Engineering nonphosphorylative metabolism to generate lignocellulose-derived products. *Nature Chemical Biology, 12(4)*, 247–253. https://doi.org/10.1038/nchembio.2020

Toivari, M. H., Nygård, Y., Penttilä, M., Ruohonen, L., & Wiebe, M. G. (2012). Microbial d-xylonate production. *Applied Microbiology and Biotechnology, 96(1)*, 1–8. https://doi.org/10.1007/s00253-012-4288-5

Toivari, M., Nygård, Y., Kumpula, E.-P., Vehkomäki, M.-L., Benčina, M., Valkonen, M., Maaheimo, H., Andberg, M., Koivula, A., Ruohonen, L., Penttilä, M., & Wiebe, M. G. (2012). Metabolic engineering of *Saccharomyces cerevisiae* for bioconversion of d-xylose to d-xylonate. *Metabolic Engineering, 14(4)*, 427–436. https://doi.org/10.1016/j.ymben.2012.03.002

Wang, J., Shen, X., Jain, R., Wang, J., Yuan, Q., & Yan, Y. (2017). Establishing a novel biosynthetic pathway for the production of 3,4-dihydroxybutyric acid from xylose in *Escherichia coli*. *Metabolic Engineering, 41*, 39–45. https://doi.org/10.1016/j.ymben.2017.03.003

Watanabe, S., Fukumori, F., Nishiwaki, H., Sakurai, Y., Tajima, K., & Watanabe, Y. (2019). Novel non-phosphorylative pathway of pentose metabolism from bacteria. *Scientific Reports, 9(1)*, 155. https://doi.org/10.1038/s41598-018-36774-6

Wei, N., Quarterman, J., Kim, S. R., Cate, J. H. D., & Jin, Y.-S. (2013). Enhanced biofuel production through coupled acetic acid and xylose consumption by engineered yeast. *Nature Communications, 4(1)*, 2580. https://doi.org/10.1038/ncomms3580

Weimberg, R., (1961). Pentose oxidation by *Pseudomonas fragi*. *J. Biol. Chem. 236*, 629–635.

Werpy, T., & Petersen, G. (2004). Top Value Added Chemicals from Biomass: Volume I -- Results of Screening for Potential Candidates from Sugars and Synthesis Gas (DOE/GO-102004-1992, 15008859). https://doi.org/10.2172/15008859

Yep, A., Kenyon, G. L., & McLeish, M. J. (2006). Determinants of substrate specificity in KdcA, a thiamin diphosphate-dependent decarboxylase. *Bioorganic Chemistry, 34(6)*, 325–336. https://doi.org/10.1016/j.bioorg.2006.08.005

Yukawa, T., Bamba, T., Guirimand, G., Matsuda, M., Hasunuma, T., & Kondo, A. (2021). Optimization of 1,2,4 - butanetriol production from xylose in *Saccharomyces cerevisiae* by metabolic engineering of NADH/NADPH balance. *Biotechnology and Bioengineering, 118(1)*, 175–185. https://doi.org/10.1002/bit.27560

669 **Table captions:**

670 **Table 1** Strain used in the present study.

671

672 **Table 2** The biochemical production by microorganisms via a xylose oxidative
673 pathway

674

675 **Figure captions:**

676 **Fig. 1**

677 Overview of the xylose oxidative pathway. KDX, 2-Keto-3-deoxy-xylonate;
678 AKGSA, α-Ketoglutarate semialdehyde; AKG, α-Ketoglutarate; EG, Ethylene
679 glycol; DHB, 3,4-Dihydroxybutanal; 3,4-DHBA, 3,4-Dihydroxybutyrate; 3-HBL, 3-
680 Hydroxybutylolactone; XylB, Xylose dehydrogenase; XylD, Xylonate
681 dehydratase; XylX, 2-Keto-3-deoxy-xylonate dehydratase; XylA, α-Ketoglutarate
682 semialdehyde dehydrogenase; YjhH and YagG, KDX aldolase, ALD, aldehyde
683 dehydrogenase; ADH, alcohol dehydrogenase; Kdc, 2-ketoacid decarboxylase.

684

685 **Fig. 2**

686 The effects of ADH gene disruption on (A) xylose consumption and (B) BT
687 production by the BDK (orange, dot circle), BDKΔ1(red, squares), BDKΔ2 (blue,
688 rhombuses), BDKΔ3 (green, triangles), BDKΔ4 (purple, crosses), BDKΔ5 (light
689 yellow, bars) BDKΔ6 (black, circles), BDKΔ7 (brown, asterisks) with disruption of
690 each ADH gene. (C) The time-course profiles of BT production and (D) 3,4-DHBA
691 production during the glucose and xylose co-fermentation by the BDδK603
692 (control, green triangles) and BDδK604 (*ADH6* deletion, red squares) strains. The
693 fermentation medium contained 10 g/L glucose and 10 g/L xylose. Error bars
694 indicate standard deviations from three independent experiments.

695

696 **Fig. 3**

697 The time-course profiles of (A) 3,4-DHBA production and (B) xylonate
698 accumulation by engineered *S. cerevisiae* strains expressing different ALDs.
699 BDδK604-YneI (blue, circles), BDδK604-Uga2 (orange, crosses), BDδK604-Ald2
700 (purple, triangles), and BDδK604-Ald3 (light yellow, asterisks). The shake-flask
701 fermentations were performed in the YP medium containing 10 g/L glucose and
702 10 g/L of xylose. (C) Time-course of pH change during the fermentation of
703 BDδK604-YneI (green). The optimal pH range of *S. cerevisiae* for growth is
704 shown in grey range. Error bars indicate standard deviations from three
705 independent experiments.

706

707 **Fig. 4**

708 The effects of different agitation rates on (A) xylose consumption, (B) xylonate
709 accumulation, and (C) 3,4-DHBA production by the BDδK604-YneI strain under
710 the pH control using a bioreactor. Agitation speeds were changed at 200 rpm
711 (orange, squares), 300 rpm (red, circles), 400 rpm (blue, rhombuses), and 500
712 rpm (green, triangles) at pH ≥ 6.0. (D) The 3-HBL productions by the BDδK604-
713 YneI strain under the different agitation speeds (200 rpm, 300 rpm, 400 rpm, and
714 500 rpm) at pH ≥ 6.0. The engineered yeast was cultivated in the YP medium
715 containing 10 g/L of glucose and 10 g/L of xylose, and the pH of fermentation
716 medium was maintained at pH ≥ 6.0 using 5 N NaOH. Error bars indicate
717 standard deviations from two independent experiments.

718

719 **Fig. 5**

720 Time-course profiles of (A) glucose consumption, (B) xylose consumption, (C)
721 xylonate accumulation, and (D) 3,4-DHBA production by the BDδK604-YneI
722 strain during the pH-controlled fermentation using a bioreactor. The

723 fermentations were performed under the alkaline conditions at pH ≥ 7.0 using
724 NaOH (orange, squares) and 8.0 using NaOH (red, rhombuses), or at pH ≥ 7.0
725 using KOH (blue, triangles), and 8.0 using KOH (green, circles) in the YP medium
726 containing 10 g/L of glucose and 10 g/L of xylose. Error bars indicate standard
727 deviations from two independent experiments.
728
729 **Fig. 6**
730 The amounts of (A) intracellular xylonate and (B) the relative amounts of
731 intracellular KDX, (C) intracellular DHB, and (D) extracellular KDX when re-
732 assimilating xylonate from the medium into the cells of the BDδK604-YneI strain.
733 The fermentations were performed at pH ≥ 7.0 or 8.0 using NaOH or KOH in the
734 YP medium containing 10 g/L of glucose and 10 g/L of xylose. Blue and orange
735 bar indicates the sample at 72 h and 96 h, respectively. The relative amounts
736 were shown as a fold change in the metabolites amount at 72 h at pH ≥ 6.0 by
737 NaOH. Error bars indicate standard deviations from two independent
738 experiments.
739

Strain Name	Description	Reference
YPH499	*MATa ura3 - 52 lys2 - 801 ade2 - 101 trp1 - 63 his3 - Δ200 le*	Stratagene
YPH499 ΔGRE3	YPH499, *gre3Δ::kanMX*	Bamba et al. 2019
BDK	YPH499, pTs-A-xylBD-kdcA	This study
BDKΔ1	BDK, *ADH1Δ::KanMX*	This study
BDKΔ2	BDK, *ADH2Δ::KanMX*	This study
BDKΔ3	BDK, *ADH3Δ::KanMX*	This study
BDKΔ4	BDK, *ADH4Δ::KanMX*	This study
BDKΔ5	BDK, *ADH5Δ::KanMX*	This study
BDKΔ6	BDK, *ADH6Δ::KanMX*	This study
BDKΔ7	BDK, *ADH7Δ::KanMX*	This study
BDδK603	YPH499 ΔGRE3, tdh3p-CcxylB, sed1p-CcxylD, six copies of *L. lactis kdcA* , *bol2Δ::HIS3* , pgk1p-tTYW1	Yukawa et al. 2021
BDδK604	BDδK603, *ADH6Δ::1 kbp fragment*	This study
BDδK604-YneI	BDδK604, pIL-tdh3p-Ec_yneI-adh1t	This study
BDδK604-Uga2	BDδK604, pIL-tdh3p-Sc_UGA2-adh1t	This study
BDδK604-Ald2	BDδK604, pIL-tdh3p-Sc_ALD2-adh1t	This study
BDδK604-Ald3	BDδK604, pIL-tdh3p-Sc_ALD3-adh1t	This study
YneI-sfpHluorin	BDδK604-YneI, pIU-pTDH3-sfpHluorin-tADH1	This study
Uga2-sfpHluorin	BDδK604-Uga2, pIU-pTDH3-sfpHluorin-tADH1	This study
Ald2-sfpHluorin	BDδK604-Ald2, pIL-pTDH3-sfpHluorin-tADH1	This study
Ald3-sfpHluorin	BDδK604-Ald3, pIL-pTDH3-sfpHluorin-tADH1	This study

Table 2 **The biochemical production by microorganisms via a xylose oxidative pathway**

Host	Carbon source	Target Products	Mode of culuture	Titer	Yield	Reference
Escherichia coli	20 g/L Xylose	3,4-DHBA	Batch, Flask	1.27 g/L	Not determined	Wang et al. 2017
Escherichia coli	5 g/L Glucose and 20 g/L Xylose	3,4-DHBA	Batch, Flask	0.38 g/L	Not determined	Gao et al. 2017
Escherichia coli	20 g/L Xylose	3,4-DHBA	Batch, Flask	7.71 g/L	60%	Liu et al. 2021
Saccharomyces cerevisiae	10 g/L glucose and 20 g/L Xylose	Glycolate	Batch, Flask	1.0 g/L	Not determined	Salusjärvi et al. 2017
Saccharomyces cerevisiae	10 g/L glucose and 10 g/L xylose	1,2,4-butanetriol	Batch, Flask	1,7 g/L	25%	Bamba et al. 2019
Saccharomyces cerevisiae	10 g/L glucose and 10 g/L xylose feeding glucose and xylose	1,2,4-butanetriol	Fed-batch, Bioreactor (pH ≥ 5.5)	6.6 g/L	57%	Yukawa et al. 2021
Saccharomyces cerevisiae	10 g/L glucose and 10 g/L xylose	3,4-DHBA, 3-HBL	Batch, Bioreactor (pH≥ 8.0)	6.5 g/L (3,4-DHBA) 0.2 g/L (3-HBL)	79%	This study

Fig. 1

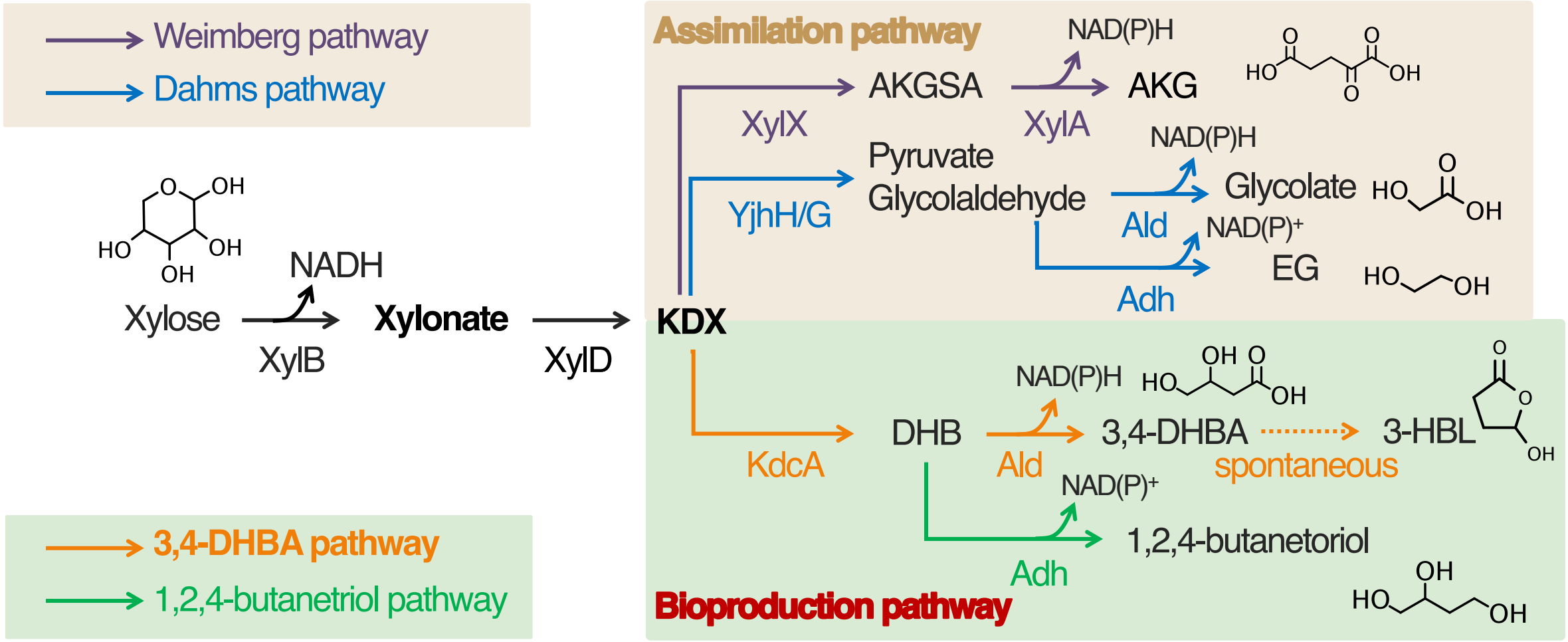
Weimberg pathway
Dahms pathway
3,4-DHBA pathway
1,2,4-butanetriol pathway
Xylose
NADH
XylB
Xylonate
XylD
KDX
Assimilation pathway
XylX
AKGSA
NAD(P)H
XylA
AKG
YjhH/G
Pyruvate
Glycolaldehyde
NAD(P)H
Ald
Glycolate
NAD(P)+
Adh
EG
KdcA
DHB
NAD(P)H
Ald
3,4-DHBA
spontaneous
3-HBL
NAD(P)+
Adh
1,2,4-butanetriol
Bioproduction pathway

Figure 2

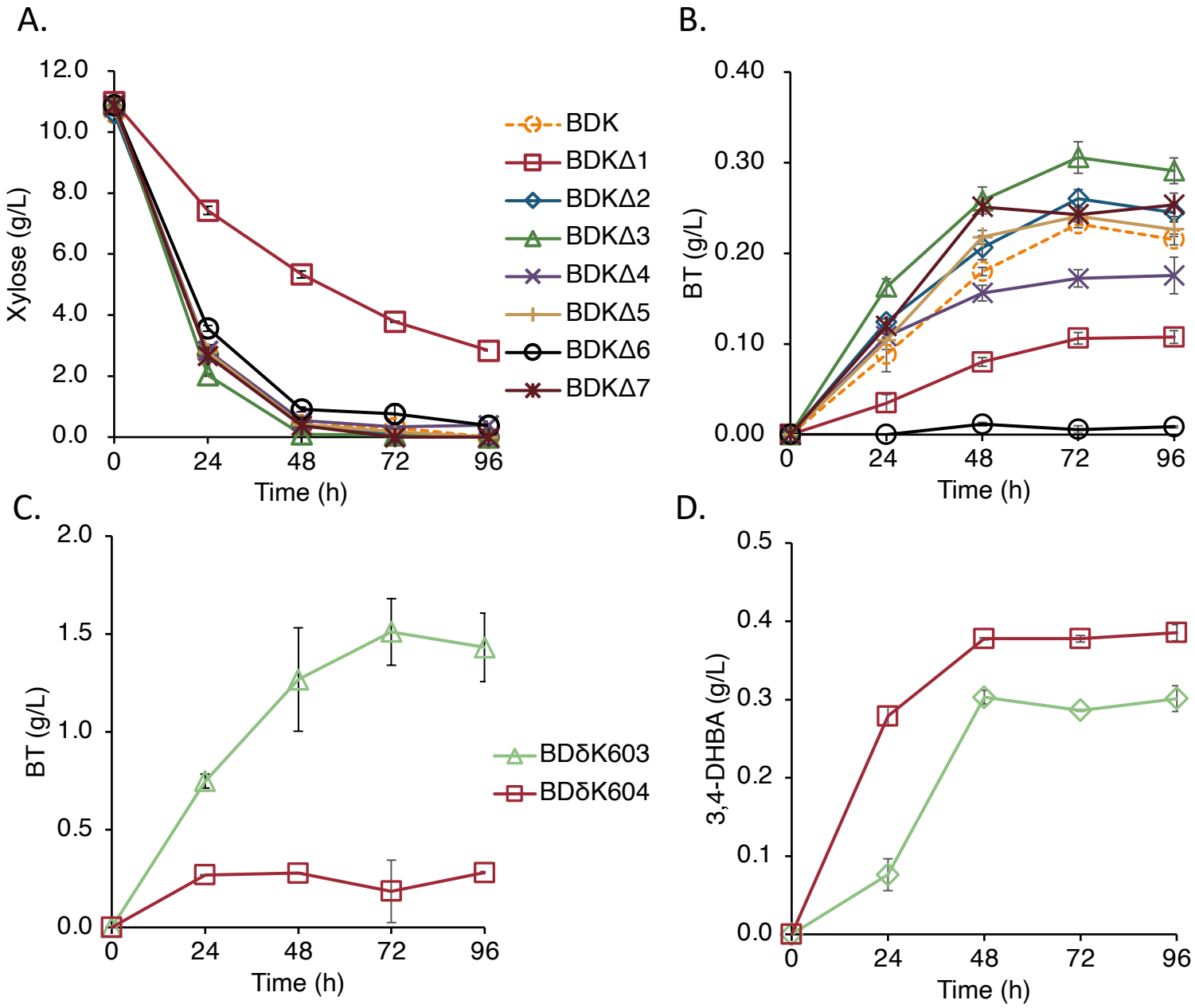
A.
Xylose (g/L)
12.0
10.0
8.0
6.0
4.0
2.0
0.0
0
24
48
72
96
Time (h)
BDK
BDKΔ1
BDKΔ2
BDKΔ3
BDKΔ4
BDKΔ5
BDKΔ6
BDKΔ7
B.
BT (g/L)
0.40
0.30
0.20
0.10
0.00
0
24
48
72
96
Time (h)
C.
BT (g/L)
2.0
1.5
1.0
0.5
0.0
0
24
48
72
96
Time (h)
BDδK603
BDδK604
D.
3,4-DHBA (g/L)
0.5
0.4
0.3
0.2
0.1
0.0
0
24
48
72
96
Time (h)

Figure 3

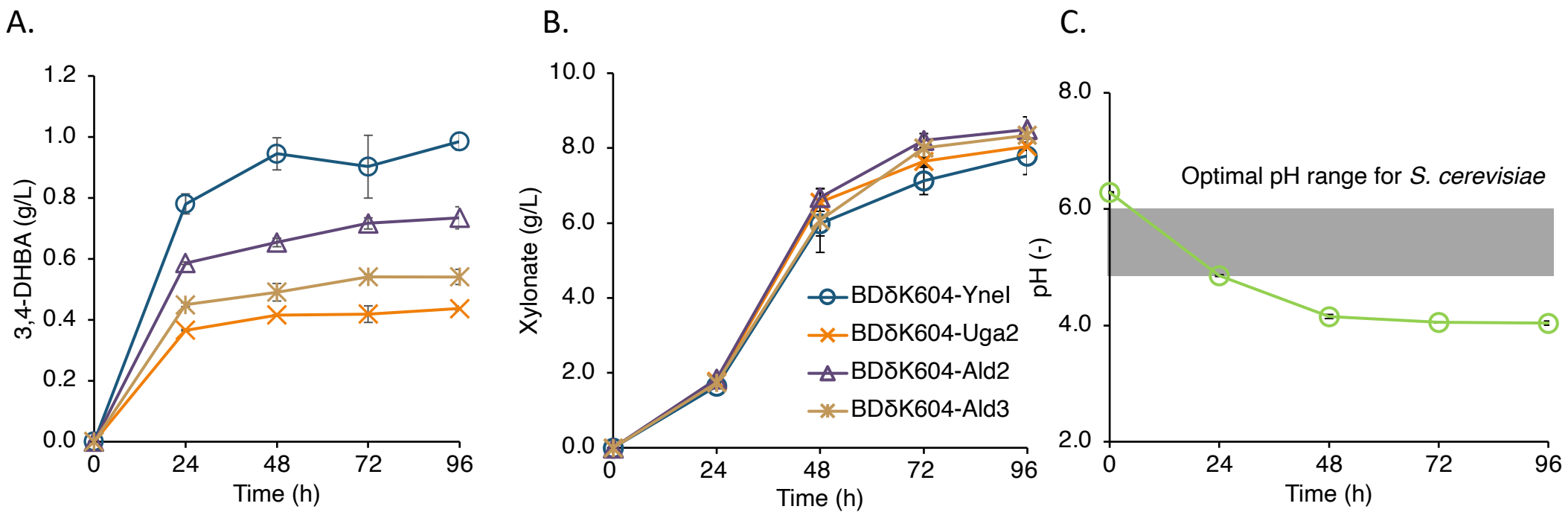
A.
3,4-DHBA (g/L)
1.2
1.0
0.8
0.6
0.4
0.2
0.0
0
24
48
72
96
Time (h)
B.
Xylonate (g/L)
10.0
8.0
6.0
4.0
2.0
0.0
0
24
48
72
96
Time (h)
BDδK604-YneI
BDδK604-Uga2
BDδK604-Ald2
BDδK604-Ald3
C.
pH (-)
8.0
6.0
4.0
2.0
Optimal pH range for *S. cerevisiae*
0
24
48
72
96
Time (h)

Figure 4

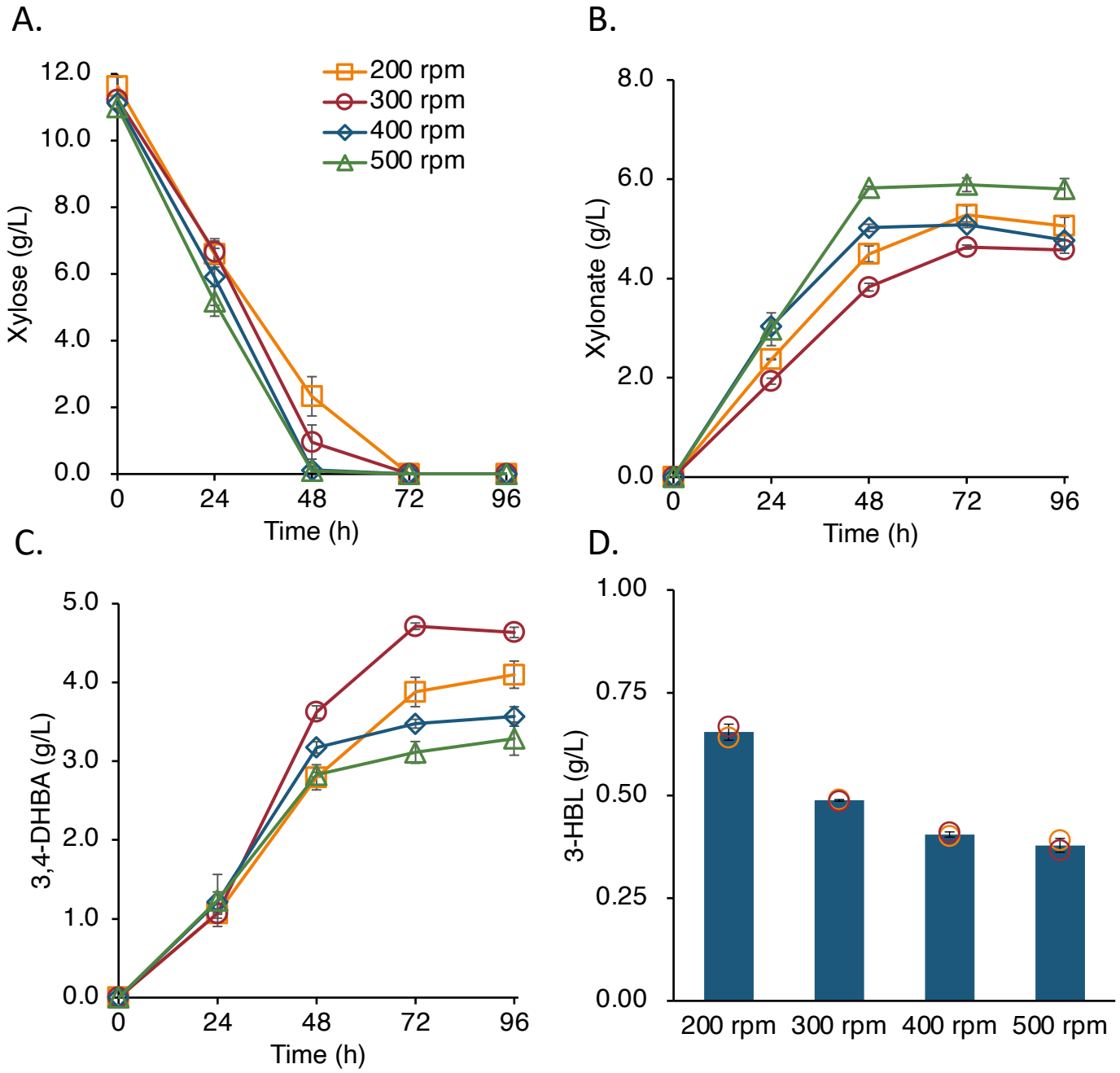
A.
B.
C.
D.
200 rpm
300 rpm
400 rpm
500 rpm
Xylose (g/L)
Xylonate (g/L)
3,4-DHBA (g/L)
3-HBL (g/L)
Time (h)
0
24
48
72
96
12.0
10.0
8.0
6.0
4.0
2.0
0.0
5.0
3.0
1.0
1.00
0.75
0.50
0.25
0.00

Figure 5

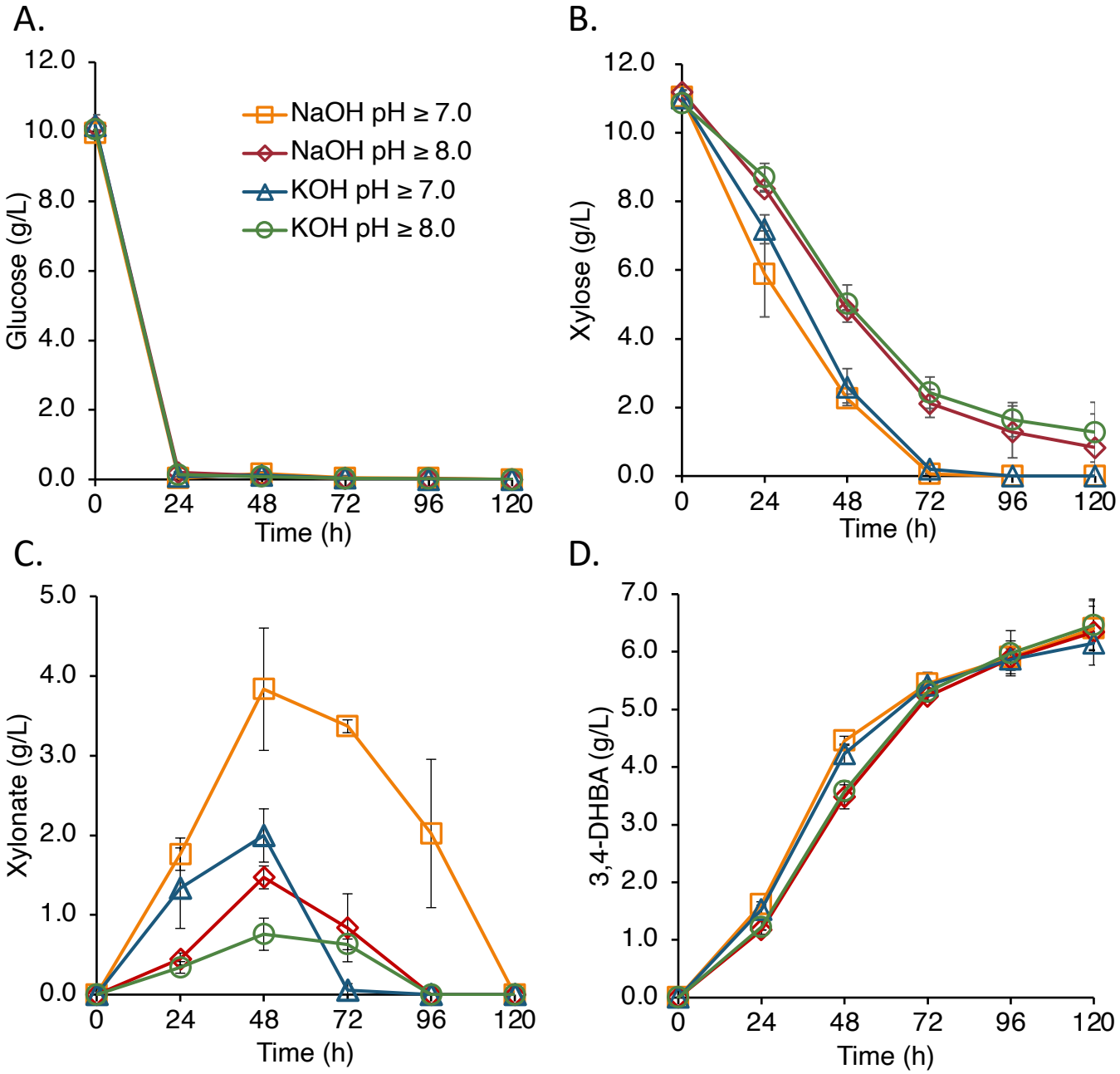
A.
B.
C.
D.
NaOH pH ≥ 7.0
NaOH pH ≥ 8.0
KOH pH ≥ 7.0
KOH pH ≥ 8.0
Glucose (g/L)
Xylose (g/L)
Xylonate (g/L)
3,4-DHBA (g/L)
Time (h)
0
24
48
72
96
120
0.0
1.0
2.0
3.0
4.0
5.0
6.0
7.0
8.0
10.0
12.0

Figure 6

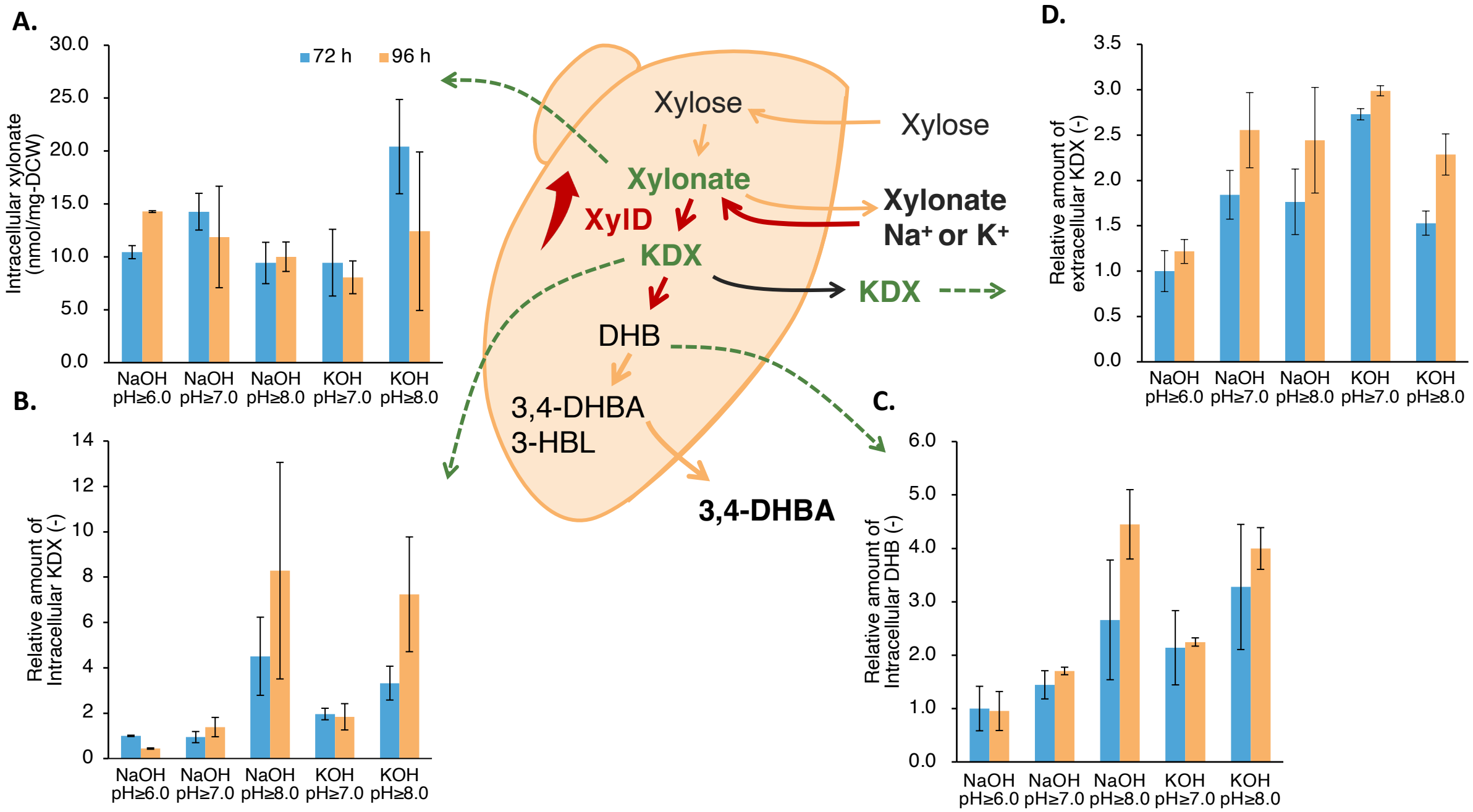
A.
72 h
96 h
Intracellular xylonate (nmol/mg-DCW)
30.0
25.0
20.0
15.0
10.0
5.0
0.0
NaOH pH≥6.0
NaOH pH≥7.0
NaOH pH≥8.0
KOH pH≥7.0
KOH pH≥8.0
B.
Relative amount of Intracellular KDX (-)
14
12
10
8
6
4
2
0
NaOH pH≥6.0
NaOH pH≥7.0
NaOH pH≥8.0
KOH pH≥7.0
KOH pH≥8.0
Xylose
Xylonate
XylD
KDX
DHB
3,4-DHBA
3-HBL
Xylose
Xylonate
Na+ or K+
KDX
3,4-DHBA
C.
Relative amount of Intracellular DHB (-)
6.0
5.0
4.0
3.0
2.0
1.0
0.0
NaOH pH≥6.0
NaOH pH≥7.0
NaOH pH≥8.0
KOH pH≥7.0
KOH pH≥8.0
D.
Relative amount of extracellular KDX (-)
3.5
3.0
2.5
2.0
1.5
1.0
0.5
0.0
NaOH pH≥6.0
NaOH pH≥7.0
NaOH pH≥8.0
KOH pH≥7.0
KOH pH≥8.0